The Role of Straining in the Electrochemical and Mechanical Behaviour of Pure Iron

M. I. Ismail* and N. Sato

Corrosion Research Group, Faculty of Engineeirng, Hokkaido University, Sapporo, Japan

(Received September, 30, 1974)

Abstract

The effect of straining and its rate on the corrosion behavior of heat treated (800°C for one hour followed by furnace cooling or water quenching) pure iron was studied by measuring the anodic current density (cd) of potentiostatically polarized specimens in 0.1 N H_2SO_4 at 20°C. Results, thus obtained, show that there are critical points in the relation, cd-strain rate. These points depend on metallurgical conditions of the metal substrate. Furnace cooled (FC) specimens have a maximum cd at a certain strain rate and passive potential (1200 mV), while at active potentials (600 mV) there exists a minimum. Water quenched (WQ) specimens always have a minimum cd at a certain rate.

In the relation of cd to strain at the same strain rate, there is a certain strain at which the average grain size of metal is larger, and at this critical strain cd is lowest (minimum). At these critical strain rates, the yield stress is also lowest (minimum), but the total strain is independent of strain rate. An identification of crystallographic, pitting and active modes of attack has been made. It is emphasized that metallographic conditions play an important role in this type of corrosion of iron.

Introduction

The effects of straining on corrosion, anodic dissolution and stress-corrosion cracking (SCC) of metals have been the subject of great interest to many investigators[1-34]. Plastic deformation or straining can result in an increase or decrease of corrosion rates; or they remain virtually unchanged[35,36]. Anodic dissolution occurs along the slip planes and the bands are formed by deformation. The amount of electric charge passed by momentary yielding is proportional to the strain[37,38]. The high rate of dissolution of bare metal will be modified by passivation and its rate[39]. Plastic deformation induces internal stresses which change the mechanical properties (e. g. increased hardness) of the metal and its susceptibility to SCC. Softening, or decrease in hardness, occurs due to relaxation processes that reduce the internal stresses. An increase in strain rate during deformation will reduce the extent of relaxation processes, and hence increases the flow stresses[40]. It is also possible to further increase the flow stresses at higher strain rates, since only an increase in force will be required to accelerate the dislocations to velocities corresponding to the appropriate strain rates. The influence of relaxation processes can be clearly established by measuring the properties of sample deformed under certain strain at various deformation rates[40].

* Permanent Address: Faculty of Engineering, Alexandria University, Egypt.

The object of this work was to investigate the influence of pre-straining rate on the electrochemical and mechanical properties of pure iron.

Experimental

Iron specimens were prepared brom 1 mm thick commercial pure iron. The composition and shape of specimens is shown in Figure 1. The specimens were mechanically polished, ultrasonically cleaned, washed and dried in usual way. Heat treatment in silica tube furnace in vaccum (10^{-3} Torr) at 800°C for an hour was followed by either slow cooling (furnace cooling, FC) or rapid cooling (ice-water cooling, WQ). In both cases the pressure inside the silica tube containing the specimens was kept always 10^{-3} Torr. Mechanically polished heat treated specimens were strained at different strain rates ($4.16\times10^{-4}S^{-1}-4.17\times10^{-1}S^{-1}$) by an Instron type testing machine. Specimens were strained till yielding and fracture. They were coated with insulating resin (inactive for electrolysis and electrolyte) except 3–4 mm area. This bare metal area and its corresponding strains ($\in=\Delta L/L_0\times100$) were determined exactly. The electrolyte (0.1 N H_2SO_4) was dearated with deoxygenated nitrogen gas[41] at 20°C. An electrolytic glass cell of 150 cc capacity, equiped with a magnetic stirrer, was used for electrolysis. A platinum plate (30 $\times$ 50 mm) was used as counter electrode. The potential of the specimen (+1200 or 600 mV, SCE) was controlled with a potentiostat (Type HP-E Nichia Keiki Co. Ltd.) referring to SCE. Current change was recorded by a chart recorder (Yokogawa Electric Works). After electrolysis the solution was analysed by an atomic absorption spectrometer (Varian Techtron Model 1100).

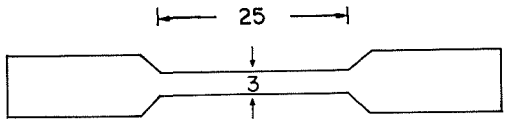

DMS in mm, Thickness = 1 mm

Test piece for tensile test

Chemical analysis according.to the supplier, (Vakkum Schmeltze G.m.b.H.), wt. %

Cr	Ni	C	Si	S	Mn	Mo	Cu	Fe
0.001	0.040	0.0035	0.008	00023	0.0005	0.001	0.002	Bal

Fig. 1 Dimensions and chemical analysis of specimens

Results

Typical current-time curves are shown in Figure 2 for various strain values and strain rates. Mostly the current densities increase with increase of strain and strain rate. Water quenched specimens (Fig. 2a) show more rapid decrease in cd with time than those that were furnace cooled (Fig. 2b). There is a sudden decrease in cd in some cases even when using active anodic potential as is clear in Figure 2c. Figure 3 shows the relation between the anodic-cd and the strain rate. For WQ specimens cd decreases with increase in strain rate to a minimum value corresponding to a certain strain rate, but for FC specimens at passive potentials (1200 mV) the reverse occurs and there is a maximum cd corresponding to a certain strain rate. Expressing the results in terms of current decay ratio (the ratio of current after 10 sec or 1 min, from the start of electrolysis to the current

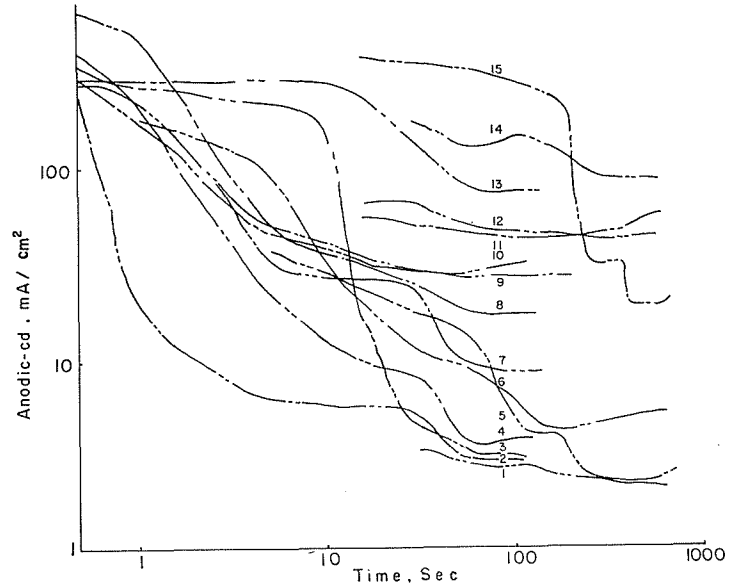

a) Rapidly cooled specimens from 800 C, 1200 mV, sce: Tensile strain, %; and strain rate, Sec^{-1}. 1, 20, $1.37\times10^{-1}S^{-1}$; 2, 25, $5\times10^{-1}S^{-1}$; 3, 80, $1.37\times10^{-1}S^{-1}$; 4, 25, $4.16\times10^{-4}S^{-1}$; 5, 20, $1.37\times10^{-1}S^{-1}$; 6, 30, $1.37\times10^{-1}S^{-1}$; 7, 30, $1.37\times10^{-1}S^{-1}$; 8, 50, $1.37\times10^{-1}S^{-1}$; 9, 20, $5\times10^{-2}S^{-1}$; 10, 30, $4.16\times10^{-4}S^{-1}$; 11, 25, $4.16\times10^{-4}S^{-1}$; 12, 50, $1.37\times10^{-1}S^{-1}$; 13, 25, $1.37\times10^{-1}S^{-1}$; 14, 80, $1.37\times10^{-1}S^{-1}$; 15, 25, $1.37\times10^{-1}S^{-1}$

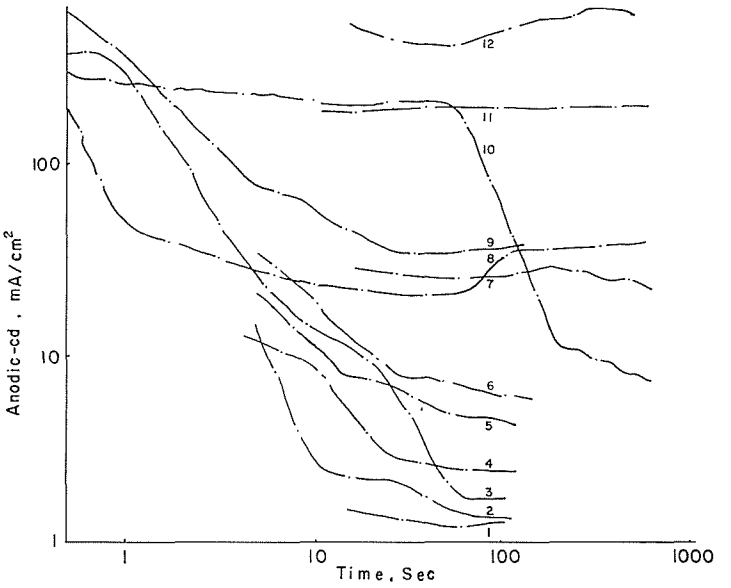

b) Slowly cooled specimens from 800 C; 1200 mV, sce: Tensile strain, %; and strain rate, Sec^{-1}. 1, 30, $4.17\times10^{-1}S^{-1}$; 2, 30, $9.33\times10^{-2}S^{-1}$; 3, 30, $4.17\times10^{-1}S^{-1}$; 4, 25, $4.77\times10^{-4}S^{-1}$; 5, 20, $9.33\times10^{-2}S^{-1}$; 6, 35, $4.77\times10^{-4}S^{-1}$; 7, 20, $4.16\times10^{-1}S^{-1}$; 8, 35, $4.77\times10^{-4}S^{-1}$; 9, 20, $4.17\times10^{-1}S^{-1}$; 10, 20, $9.33\times10^{-2}S^{-1}$; 11, 225, $4.77\times10^{-4}S^{-1}$; 12, 30, $9.33\times10^{-2}S^{-1}$

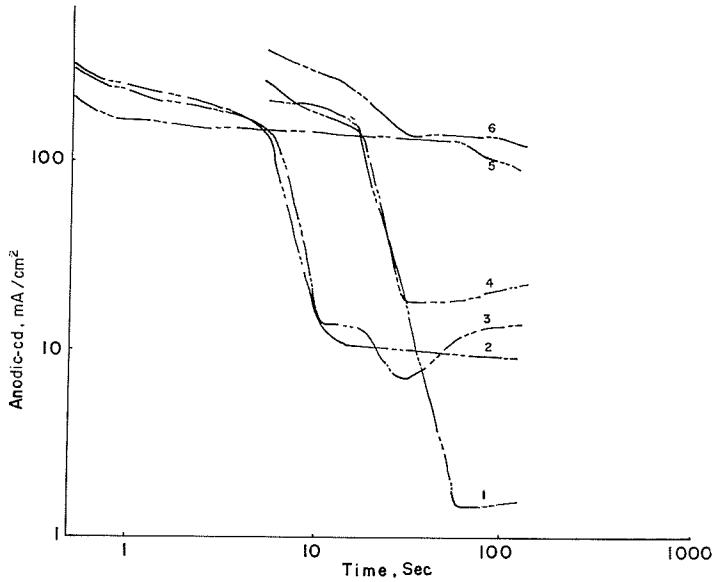

c) Rapidly cooled specimens from 800 C; 600 mV, sce: Tesile strain, %; and strain rate, Sec^{-1}. 1, 25, $5\times10^{-2}S^{-1}$; 2, 30, $1.37\times10^{-1}S^{-1}$; 3, 30, $1.37\times10^{-1}S^{-1}$; 4, 50, $1.37\times10^{-1}S^{-1}$; 5, 25, $4.16\times10^{-4}S^{-1}$; and 6, 20, $5\times10^{-2}S^{-1}$

Fig. 2 Potentiostatic current density-time curves for pre-strained heat treated iron at different anodic potentials, strains, and strain rates in 0.1 N sulfuric acid at 20 C

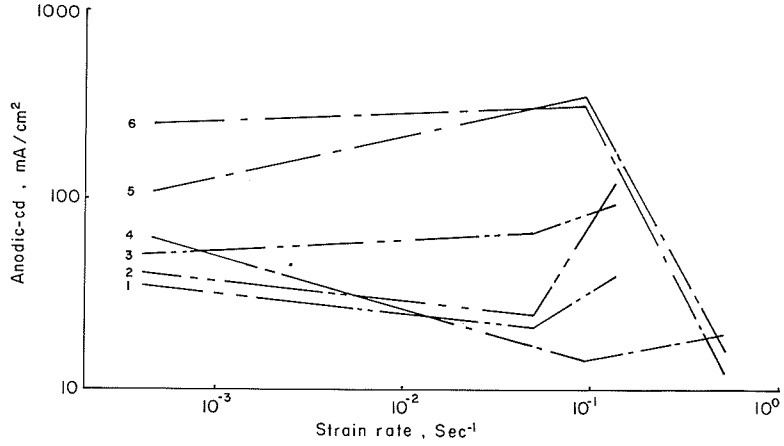

Fig. 3 Current density vs strain rate at constant strain (30%) in 0.1 N H_2SO_4 at 20 C. Rate of cooling from 800 C (rapid, WQ, or slow,FC); polarization time, min; and potential, mV, sce. 1, WQ, 10, 1200; 2, WQ, 2, 600; 3, WQ, 2, 600; 4, FC, 2, 600; 5, FC, 2, 1200; and 6, FC, 10, 1200

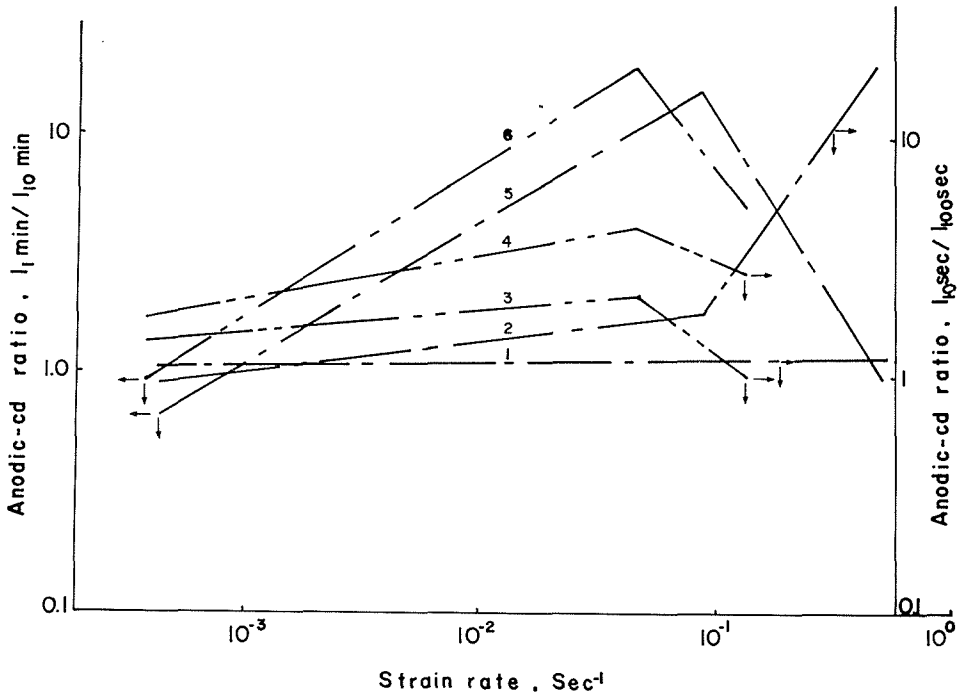

Fig. 4 Plot of current decay ratio (I_{10sec}/I_{100sec} and I_{1min}/I_{10min}) against strain rate in 0.1 N H_2SO_4 at 20 C. Rate of cooling from heat treatment temperature (800 C); polarization potential, mV, sce: 1, FC, 1200; 2, FC, 600; 3, WQ, 600; 4, WQ, 1200; 5, FC, 1200; and 6, WQ, 1200

after 100 sec, or 10 min, respectively) in relation to strain rate, Figure 4 demonstrated that there is a maximum current decay ratio at a certain strain rate. This depends on the metallurgical conditions of metal substrate. This maximum is higher for WQ specimens and occurs at a slightly lower strain rate than those of FC specimens. In the earlier stages (10–100 sec) the strain rates have no effect on dissolution of FC specimens at 1200 mV, but at 600 mV there is an increase in the current decay ratio leading to inactive dissolution or passivation, despite the active potential used during polarization. The relationship between cd, grain size, and strain rate were studied. The mean size of subgrains obtained after deformation at a given strain rate was determined by measuring the average diameter of the grains. The results are represented graphically in Figure 5. Figure 5a indicates that at a certain critical strain there is a decreaseto a minimum of current density and an increase to a critical maximum in the average size of the deformed grains. This behaviour indicates that a relationship exists between grain size and current density, as the larger grain size corresponds to the lower current density. The straining rates affects the value of critical grain size. Lower strain rates result in the formation of smaller critical grain size and consequently higher current density. The value of this cd decreases with increase of strain (Fig. 5b).

Atomic absorption spectrophotometric analysis of the electrolyte after polarization, as shown in Figure 6, indicated that for WQ specimens the amount of dissolved metal (Fe^{2+}) in the solution increases with increase of strain rate, while the amount of metal dissolved from the FC specimens is not sensitive to the lower

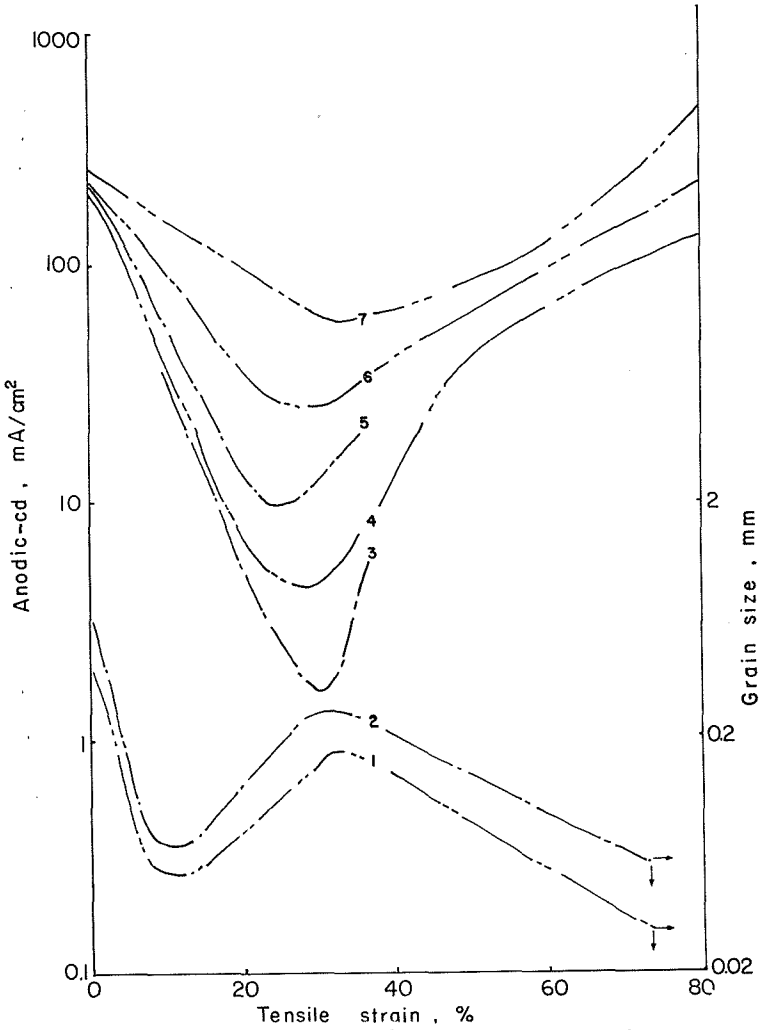

a) Strain rate=1.37×10^{-1}Sec^{-1}: 1, WQ, 2, FC; 3, FC; 4, WQ; 5, FC; 6, WQ; and 7, WQ. Polarization time, Sec: 7, 1; 6 and 5, 10; 4 and 3, 100

strain rates, but, rather decreases at higher strain rates. FC specimens giving a large amount of dissolved metal, corrode more than the WQ ones. The influence of strain rate on the behaviour of metal during straining is shown in Figure 7. At low strain rates WQ specimens yield at higher values than the FC, but at high strain rates FC specimens have higher yield stress. Curve shape reflects the plastic deformation mechanism of the specimens. The total strain of specimens is insensitive to strain rate for FC while for WQ specimens it decreases with increase of strain rate, as shown in Figure 8. The yield stress decreases to a minimum value with increase of strain rate. The time elapsed before specimen fracture is inversally proportional to the strain rate.

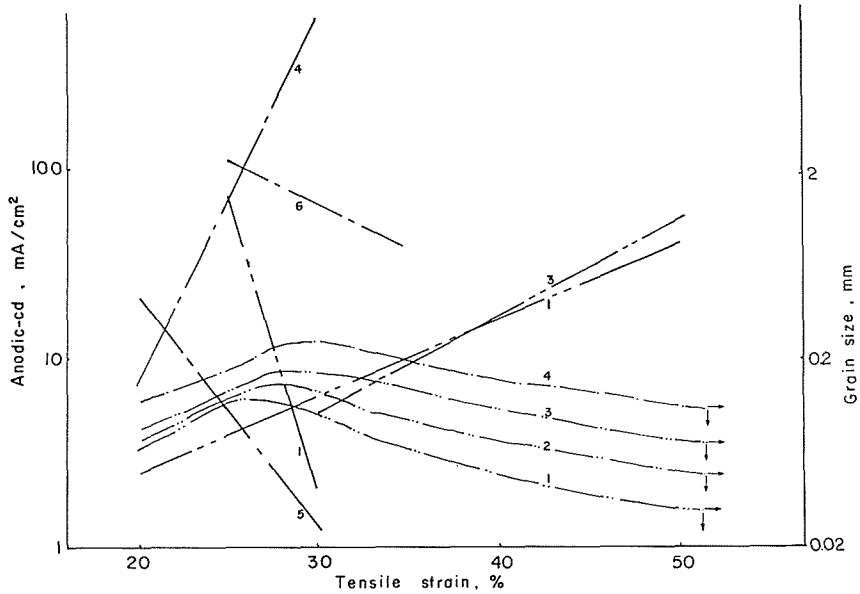

b) Polarization time=10 min: rate of cooling; strain rate; 1, WQ, $4.16\times10^{-4}S^{-1}$; 2, WQ, $5\times10^{-2}S^{-1}$; 3, WQ, $1.37\times10^{-1}S^{-1}$; 4, FC, $6.33\times10^{-2}S^{-1}$; 5, FC, $4.17\times10^{-1}S^{-1}$; and 6, FC, $4.77\times10^{-4}S^{-1}$

Fig. 5 Current desity, strain and grain size relationship in 0.1 N H_2SO_4 at 20 C and 1200 mV, sce. Heat treatment cycle: 1 hour at 800 C; rapid cooling, WQ, or slow cooling, FC

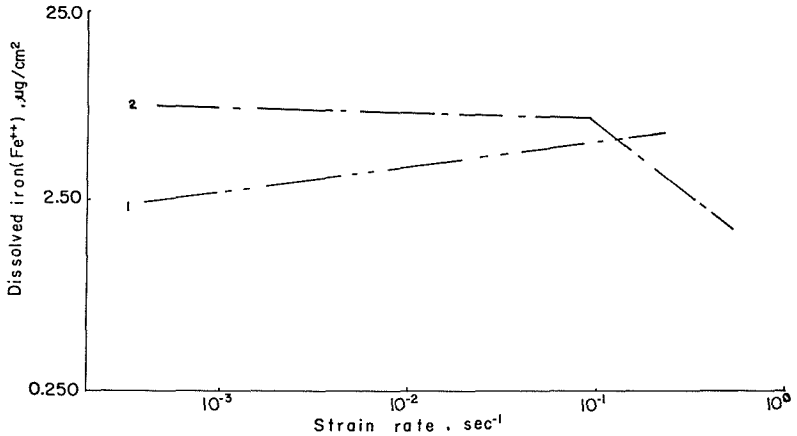

Fig. 6 Amount of iron dissolved (Fe^{2+}) during potentiostatic polarization in 0.1 N H_2SO_4 at 1200 mV and at strain=30%. 1, specimen rapidly cooled from 800 C; 2, specimen slowly cooled

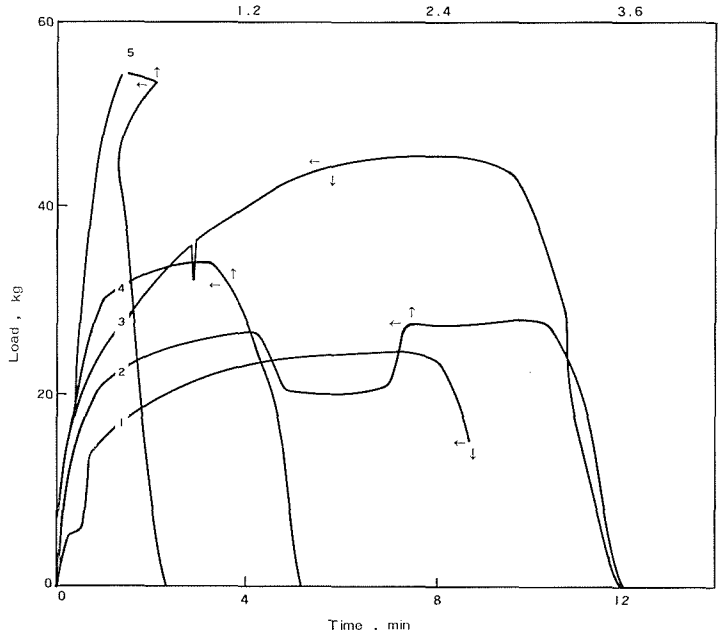

Fig. 7 Load-time curves of iron during deformation at different tensile strain rates. Rate of cooling, strain rate: 1, FC, $4.77\times10^{-4}S^{-1}$; 2, FC, $9.33\times10^{-2}S^{-1}$; 3, WQ, $4.16\times10^{-4}S^{-1}$; 4, WQ, $1.37\times10^{-1}S^{-1}$; and 5, FC, $4.17\times10^{-1}S^{-1}$

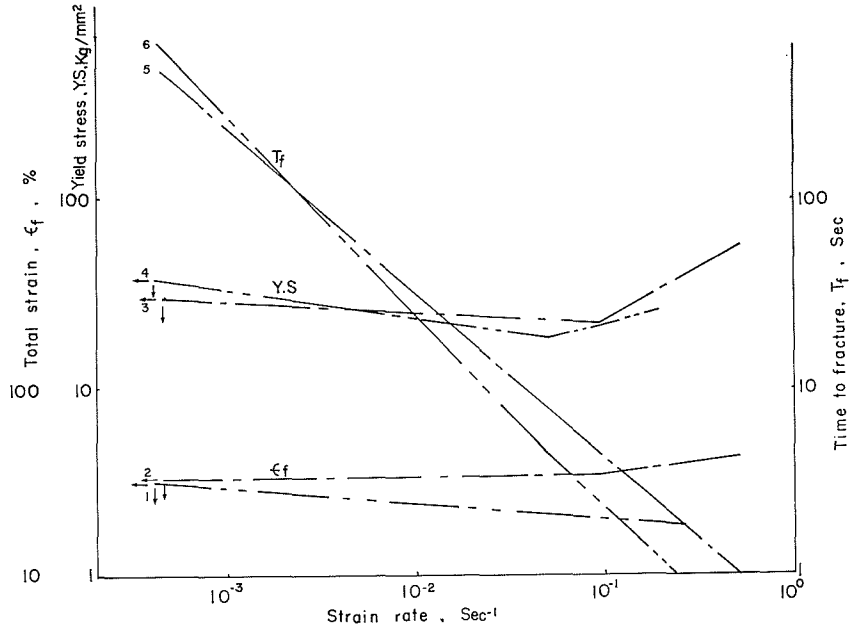

Fig. 8 Influence of strain rate on mechanical properties of iron. Rate of cooling from 800 C; property: 1, WQ, total strain; 2, FC, total strein; 3, FC, yield stress; 5, FC, time to fracture in tension; and 6, WQ, time to fracture in tension

Discussion

There are several reports available in the literature dealing with the effect of straining on corrosion and dissolution of metals. The effect have been described as an increase in metal dissolution rate as a result of the effect of active atoms (loosely bound) present around the deformed grain boundaries[26]. Yielding of metals has also been found to be accompanied by an increase in anodic-cd at constant anodic potential[9]. The increase in the member of active sites on the surface results in an increase of the dissolution of this surface. The balance between the rate of creation of new active sites and the rate of their disappearance by dissolu-

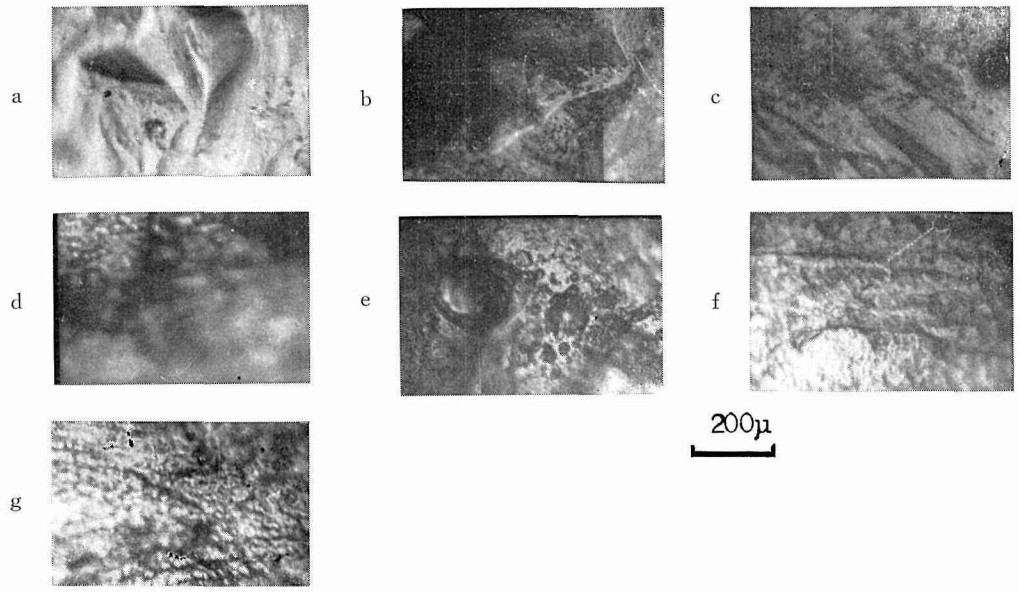

a) Slowly cooled specimens from 800 C (0.001 C/Sec). Tensile strain, %, strain rate, Sec^{-1}: a, 20, 4.77×10^{-4}; b, 40, 4.77×10^{-4}; c, 60, 4.77×10^{-4}; d, 20, 9.33×10^{-2}; e, 30, 9.33×10^{-2}; f, 30, 4.17×10^{-1}; and g, 20, 4.17×10^{-1}

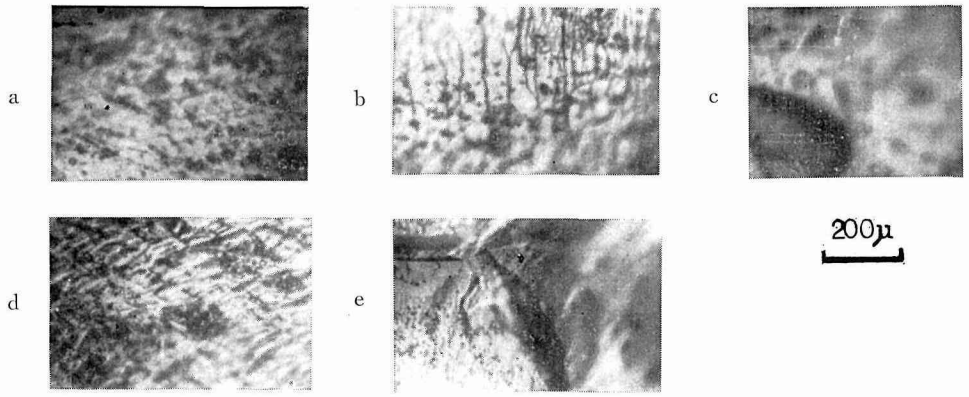

b) Rapidly cooled specimens from 800 C (100 C/Sec). Tensile strain, %; strain $rate^{-1}$: a, 25, 4.16×10^{-4}; b, 30, 4.16×10^{-4}; c, 50, 5×10^{-2}; d, 25, 1.37×10^{-1}; and e, 80, 1.37×10^{-1}

Fig. 9 Microstructure of iron specimens strained with different strain rates to different strains

tion or passivation determines the final decrease or increase of anodic-cd. It is well known that active surface corresponds to numerous high index planes that have emerged by slipping[35,36]. But the true mechanism is not yet well understood particularly since the kinetics of the process is complicated by the simultaneous dissolution and film formation at the surface. Active dissolution rates on low-index planes are normally slower than those on high-index planes[42], although in the potential region where the film formation process becomes possible the opposite may be true[43]. Kruger[44] has observed, by optical and transmission electron microscopy, non continuous cathodic sites on iron that has been passivated and then placed in a dilute copper sulfate solution until passivity had decayed, as indicated by potential measurements. It was determined indirectly (through copper deposition at the cathodc sites during the attack on the passive film) that the breakdown depends on the properties of the passivating film. In turn these are affected by the metal surface since surface orientation influences the number of breakdown sites[44]. In contradiction to Kruger's results, a nucleation of film breakdown independent of substrate orientation was indicated by Pickering and Frankenthal[43] in their studies on Fe-Cr system.

After the application of voltage, the current is found to decrease in the process of anodic dissolution of iron at constant potential in sulfuric acid. After some time it goes through a minimum and increases again till a constant value is attained. The initial decrease of the current is known to be associated with the formation of surface oxide film. The increase in the current after it reaches minimum value, is caused by the formation of pores (Fig. 9). These pores may be formed due to active pitting in the film or local dissolution of the oxide film. In a recent review on break down of anodic oxide films on metals Sato[45] discussed the pore formation and transpassive dissolution of anodic oxides. The rate of dissolution from the pore base is sometimes hundreds or thousands of times larger at the pore base than at the wall[46,47].

Metal substrate dislocation plays an important role in metal dissolution and in mechanical behaviours. Metal substrate grain size gives an indication of the dislocation density at the subgrain boundary, as the latter is calculated from subgrain size and the misorientation angle, between the subgrains. It is of interest to correlate the yield stress of the deformed metal to its dislocation structure as the theories of metal strenghing relate flowstress value to dislocation density[48]. Large slipping rate occurs at yielding of the metal, and the emerging active surface, which has highly activated atoms, provides an increased dissolution rate. Defects formed by yielding control the activity of adatoms on active surfaces. An active surface is deactivated by the disappearance of the defect due to the preferential dissolution. Hoar and Jones[3] in a recent report on straining of mild steel in boiling sodium hydroxide solution suggested that the increase of current density is due to rupture of the protective surface film. They also mentioned the possibility that the dissolution of bare metal is not strain-accelerated. Experimental results indicated that the total strain attained by iron before its failure in tension is approximately constant and not greatly affected by strain rate. This is in accordance with a recent work on Copper[4].

Current change observed upon straining of iron in a film forming solution can be analyzed in terms of the summation of individual current and decay associated with oxide rupture followed by passivation at emergent slip steps[6]. Steady current value may occur when the rate of passivation of a corroding surface is equal to the rate of creation of new active surface.

Concluding Remarks

1. The increase in straining rate induces internal stresses which lead to an increase in corrosion (cd). There is a critical strain rate whose value depands on the metallurgical condition of the speicmen. This critical strain rate corresponds to critical points in the strain rate-property curves.

2. Current decay rate is larger for WQ than for FC specimens. There is also a maximum at the critical strain rate, but in the initial stage, (10–100 sec), the current decay rate does not depend on strain rate for FC specimens.

3. Generally the anodic-cd increases with strain but for very solw rates of strain, it decreases in the range of strain 20–30%.

4. The amount of dissolved iron is affected by metallurgical condition and strain rate. There is a critical strain at which a decrease occurs. There is a decrease in this amount from FC specimens while an increase from WQ. This behaviour may be due to the morphology of surface attack since WQ specimens are smoothly passivated and all of the corroded metal stays in solution, while, in contrast, the FC specimens show pitting and there are deposited corrosion products which lead to a decrease in dissolved metal (Fig. 9).

5. Mechanical properties are largely affected by strain rate. Yield stress has a minimum at the critical strain rate, while the time required for fracture directly decreases with strain rate. The overall strain is only slightly affected by strain rates.

We have further used the present technique to examine the influence of heat-treatment on the susceptibility towards SCC of iron in H_2SO_4, the results will be reported later.

Acknowledgement

We gratefuly acknowledge the Japan Society for the Promotion of Science (JSPS) for a post-doctoral fellowhsip provided for one of us (M. I. I.) during the tenure of which this work was carried out.

References

1) Shibata, T., Takeyama, T.: Boshoku Gijutsu, 23 (1974), p. 379.
2) Shibata, T., Takeyama, T.: Japan Inst. Metals 38, (1974), 2, p. 125.
3) Hoar, T. P., and Jones, R. W.: Corros. Sci, 13, (1973), p. 725.
4) Haruyama, S., and Asawa, S.: Corros. Sci. 13, (1973), p. 395.
5) Asawa, S., Haruyama, S. and Nagasaki, K.: Japan Inst. Metals, 36 (1972), 5, p. 440.
6) Hoar, T. P., and Ford, F. P.: J. Electrochem. Soc., 120 (1973), 8, p. 1013.
7) France, W. D.: Corrosion, 26, (1970), 5, p. 189.
8) Hoar, T. P., Podesta, J. J. and Rothwell, G. P.: Corros. Sci., 11 (1971), p. 231.
9) Hoar, T. P. anc Galvele, J. R.: Corros. Sci. 10, (19707), p. 211.
10) Lewis, D., Northwood, D. O. and Pearce, C. E.: Corros. Sci. 9 (1969), p. 779.
11) Trabanelli, G., Zucchi, F.: Electrochim. Metal., 1. (1966), p. 251.
12) Long, L. M. and Uhlig, H. H.: J. Electrochem. Soc. 112 (1965), p. 965.
13) Tomashov, N. D., and Ivanov, Y. M.: Zashchita Metallov, 1, (1965), p. 36.
14) Foroulis, Z. A., and Uhlig, H. H.: J. Electrochem. Soc., 111, (1964), p. 522.
15) Windfeldt, A.: Electrochim. Acta, 9, (1964), p. 1139.
16) Greene, N. D., and Saltzman, G. A.: Corrosion 20 (1964), p. 293t.
17) Hoar, T. P., and Scully, J. C.: J. Electrochem. Soc.,: 111, (1964), p. 348.
18) Hoar, T. P.: Corrosion, 19 (1963), p. 311t.

19) Hoar, T. P., and West, J. M.: Proc. R. Soc., A286 (1962), p. 304.
20) Giddings, J. C., Funk, A. G., Christensen, C. J., and Eyring, H.: J. Electrochem. Soc. (1959), p. 91.
21) Hoar, T. P., and West, J. M.: 181 (1958), p. 835.
22) Straumanis, M. E., and Wang, Y. N.: Corrosion, 12, (1956), p. 177t.
23) Hoar, T. P., and Hines, J. G.: Stress Corrosion Cracking and Embrittlement, (1956), p. 107, Wiley.
24) Hoar, T. P., and Hines, J. G.: J. Iron Steel Inst. 182 (1956), p. 124.
25) Logan, H. L.: J. Res. Natn. Bur. Stand, 48, (1955), p. 99.
26) Gerischer, H., and Rickert, H.: Z. Metallk. 46, (1955), p. 681.
27) Simnad, M. T., and Evans, U. R.: Faraday Soc., 46 (1950), p. 175.
28) Copson, H. R.: Stress Corrosion, The Corrosion Handbook, (1948), p. 569, Uhlig, H. H. ed., Wiley & Sons.
29) Franks, R.: Chromium-Nickel Austenitic Stainless Steels; The Corrosion Handbook, Uhlig, H. H., ed. (1948), p. 150, Wiley & Sons.
30) Garre, B.: Korrosion u. Metallsch, 6, (1930), p. 200.
31) Heyn, E., and Bauer, O.: J. Iron and Steel Inst., 79 (1909), p. 109.
32) Walker, W. H., and Dill, C.: Proc. Am. Soc. Testing Materials, 7 (1907), p. 230.
33) Hambuechen, Bulletin, University of Wisconsin, Engineering Series, No. 8 (1900), see also ref. 3.
34) Andrews, T.: Proc. Inst. Civil Engrs, 118 (1894), p. 356, see also ref. 3.
35) Despic, A. R., Raicheff, R. G., and Bockris, J.O'M.: J. Chem. Phys. 49, (1967), p. 926.
36) Raicheff, R. G., Damjanovic, A., and Bockris, J. O'M.: J. Chem. Phys., 47 (1967), p. 2198.
37) Asawa, S., Haruyama, S., and Nagasaki, K.: J. Japan Inst. Metals, 36 (1972), p. 440.
38) Haruyama, S., Asawa, S., and Nagasaki, K.: Denki Kagaku, 39 (1971), p. 564.
39) Logan, H. L.: J. Res. Nat. Bur. Std. 48 (1952), p. 99.
40) Korbel, A., and Swiatkowski, K.: Net. Sci. J., J. The Inst. Met., 6 (1972), p. 60.
41) Humphries, M. J., and Parkins, R. N.: Corros. Sci., 7, (1967), 747.
42) Despic, A. R., Raicheff, R., and Bockris, J. O'M.: J. Chem. Phys., 49 (1968), p. 926.
43) Pickering, H. W., and Frankenthal, R. P.: J. Electrochem. Soc., 112 (1965), p. 761.
44) Kruger, J.: J. Electrochem. Soc., 110 (1963), p. 654.
45) Sato, N.: Electrochim. Acta, 16 (1971), p. 1683.
46) Nagayama, M., and Tamura, K.: Electrochim. Acta, 12 (1967), p. 1097.
47) Nagayama, M., and Tamura, K.: Electrochim. Acta, 13 (1968), p. 1773.
48) Friedel, J.: Dislocations (1966), Pergamon Press.